



*DEFENSE & SECURITY SOLUTIONS*

**KRATOS**  
FROM STRENGTH TO SUCCESS™



Wide-field Imaging System and Rapid Direction of Optical Zoom (WOZ)  
(Contract Number N00014-10-C-0194)

Quarterly Technical Report #3  
16 Dec 2010 - 15 Mar 2011

Submitted by  
Kratos Defense and Security Solutions

Prepared by  
Dr. Greg A. Finney

Sponsored by  
Office of Naval Research  
Code 312

25 Mar 2011

Unclassified/Distribution Unlimited

## Report Documentation Page

*Form Approved*  
*OMB No. 0704-0188*

Public reporting burden for the collection of information is estimated to average 1 hour per response, including the time for reviewing instructions, searching existing data sources, gathering and maintaining the data needed, and completing and reviewing the collection of information. Send comments regarding this burden estimate or any other aspect of this collection of information, including suggestions for reducing this burden, to Washington Headquarters Services, Directorate for Information Operations and Reports, 1215 Jefferson Davis Highway, Suite 1204, Arlington VA 22202-4302. Respondents should be aware that notwithstanding any other provision of law, no person shall be subject to a penalty for failing to comply with a collection of information if it does not display a currently valid OMB control number.

1. REPORT DATE <b>15 MAR 2011</b>	2. REPORT TYPE	3. DATES COVERED <b>00-00-2011 to 00-00-2011</b>			
4. TITLE AND SUBTITLE <b>Wide-field Imaging System And Rapid Direction Of Optical Zoom (WOZ)</b>		5a. CONTRACT NUMBER			
		5b. GRANT NUMBER			
		5c. PROGRAM ELEMENT NUMBER			
6. AUTHOR(S)		5d. PROJECT NUMBER			
		5e. TASK NUMBER			
		5f. WORK UNIT NUMBER			
7. PERFORMING ORGANIZATION NAME(S) AND ADDRESS(ES) <b>Kratos Defense and Security Solutions, 4820 Eastgate Mall, San Diego, CA, 92121</b>		8. PERFORMING ORGANIZATION REPORT NUMBER			
9. SPONSORING/MONITORING AGENCY NAME(S) AND ADDRESS(ES)		10. SPONSOR/MONITOR'S ACRONYM(S)			
		11. SPONSOR/MONITOR'S REPORT NUMBER(S)			
12. DISTRIBUTION/AVAILABILITY STATEMENT <b>Approved for public release; distribution unlimited</b>					
13. SUPPLEMENTARY NOTES					
14. ABSTRACT <b>This report covers technical progress on the Wide-field Imaging System and Rapid Direction of Optical Zoom (WOZ) contract for the period 16 Dec 2010 - 15 Mar 2011. A report covering financial status for this period is provided separately. During this period, the multiphysics design tool has been further developed and is nearing completion. A substantial amount of testing on the initial materials samples has revealed several characteristics which are not yet well understood. The set of material characterization samples has been fabricated by NeXolve and will undergo additional processing in the coming quarter.</b>					
15. SUBJECT TERMS					
16. SECURITY CLASSIFICATION OF:			17. LIMITATION OF ABSTRACT <b>Same as Report (SAR)</b>	18. NUMBER OF PAGES <b>16</b>	19a. NAME OF RESPONSIBLE PERSON
a. REPORT <b>unclassified</b>	b. ABSTRACT <b>unclassified</b>	c. THIS PAGE <b>unclassified</b>			

Quarterly Technical Report #3 (QTR-3)

**Wide-field Imaging System and Rapid Direction of Optical Zoom (WOZ)  
QTR-3**

Contract Number  
N00014-10-C-0194

Prepared for  
Office of Naval Research Code 312

Covering the Period  
16 Dec 2010 - 15 Mar 2011

Submitted by  
Dr. Greg A. Finney, Principal Investigator  
Kratos Defense and Security Solutions/Digital Fusion  
Sensors & Space Systems Group

Keywords:  
Flexible membranes, optics, polyvinylidene fluoride

Distribution:  
Distribution A. Approved for public release; distribution is unlimited.

## **Abstract**

This report covers technical progress on the Wide-field Imaging System and Rapid Direction of Optical Zoom (WOZ) contract for the period 16 Dec 2010 - 15 Mar 2011. A report covering financial status for this period is provided separately. During this period, the multiphysics design tool has been further developed and is nearing completion. A substantial amount of testing on the initial materials samples has revealed several characteristics which are not yet well understood. The set of material characterization samples has been fabricated by NeXolve and will undergo additional processing in the coming quarter.

## Figures

Figure 1. Example electrode pattern from script within the multiphysics tool	3
Figure 2. Tip response to alternating 0 and 2kV voltage, 10.6 cm length (above) and 3.8 cm length (below)	4
Figure 3. Film loaded in Instron tensile tester with connections to the current integrator	5
Figure 4. Load - extension graph for 69 um film loaded at 0.05 mm/s	6
Figure 5. Current integrator counts vs. applied tensile load for the same test as Figure 3	7
Figure 6. Schematic diagram for capacitance measurement	8
Figure 7. Test setup measuring response to lateral loads	9
Figure 8. Charge generated by bending bimorph strip	9

## Contents

Abstract	iii
Figures	iv
Summary	1
Introduction	1
Methods, Assumptions, and Procedures	1
Analytical and Numerical Model	1
Experimental Testing	3
Applied Voltage	4
Applied Load	5
Dielectric Constant	7
Results and Discussion	9
Conclusions	11

## **Summary**

In June 2010, Digital Fusion Solutions (DFS, a wholly-owned subsidiary of Kratos Defense and Security Solutions, Inc.) was awarded a contract for the development of optical quality flexible membrane mirrors. This report covers technical progress on the Wide-field Imaging System and Rapid Direction of Optical Zoom (WOZ) contract for the period 16 Dec 2010 - 15 Mar 2011. A report covering financial status for this period is provided separately. During this period, the multiphysics design tool has been further developed and is nearing completion. A substantial amount of testing on the initial materials samples has revealed several characteristics which are not yet well understood. The set of material characterization samples has been fabricated by NeXolve and will undergo additional processing in the coming quarter.

## **Introduction**

DFS has teamed with Advanced Optical Systems, Inc (AOS) and NeXolve, Inc. to develop a breadboard system for demonstrating non-mechanical zoom using flexible thin films. The project consists of three major task area, which are Material Characterization, Diagnostic System Development, and Imaging System Development. DFS is responsible for leading the modeling effort, AOS is responsible for leading the optical design effort, and NeXolve is responsible for fabrication of the films. In addition, each member of the team supports the others in their areas of responsibility.

Material Characterization phase will involve two components: development of modeling tools and measurement of material properties for use in the tools. This phase is currently ongoing and will be discussed thoroughly in the next section. The Diagnostic System Development phase will apply the tools and knowledge developed in the first phase to build algorithms for modeling and testing one-dimensional films with multiple actuators. These models will then be compared to experimental results and modified as needed. The Imaging System Development phase will conclude the effort by building a sensor system with variable zoom based on optical quality PVDF films.

## **Methods, Assumptions, and Procedures**

The modeling tools are based on interaction between three commercial software packages: SolidWorks, COMSOL Multiphysics, and ZEMAX optical design. The multiphysics design tool is nearing completion. We have demonstrated the ability to create a model in SolidWorks, import the model into COMSOL, and then interactively update the model with either package. COMSOL can then perform the electrostatic and mechanical modeling to calculate the deformation resulting from the applied voltages. Finally, the deformed surface can be exported to ZEMAX via MatLab. From ZEMAX, various analyses can be conducted to determine important parameters such as focal point, aberrations, and wavefront distortion. Defining the specific analytical results to extract from ZEMAX to support the optimization remains to be determined.

### ***Analytical and Numerical Model***

An analytical model was developed to determine the relationship between the curvature of a clamped cantilever beam and the voltage applied. A model for a bimorph piezoelectric

structure from the literature was used to compare the results with the numerical results from COMSOL. From Smits,<sup>1</sup> an expression for the displacement,  $\delta$ , is given by

$$\delta = \frac{L^3 F}{2Ewh^3} + \frac{3d_{31}L^2 V}{8h^2}, \quad (1)$$

where  $L$  is the length of the film,  $w$  is the width of the film,  $h$  is the thickness of each layer of the bimorph,  $E$  is Young's modulus,  $d_{31}$  is the piezoelectric coefficient relating the strain in the  $x$  direction to the field in the  $z$  (thickness) direction,  $F$  is the applied force, and  $V$  is the applied voltage.

**Table 1. Comparison of numerical and analytical results for bimorph cantilever with applied force and voltage**

Inputs		Outputs	
		Displacement (mm)	
Voltage (V)	Force (N)	Numerical	Analytical
20000	0	32.812	32.812
0	-0.00152	-32.716	-32.803
2000	-0.00152	0.097	0.010

Again, following Smits, the charge,  $Q$ , generated on each surface from an applied force is given by

$$Q = \frac{3d_{31}L^2 F}{8h^2}, \quad (2)$$

Substituting  $\delta = \frac{L^3 F}{2Ewh^3} + \frac{3d_{31}L^2 V}{8h^2}$ , (Eq. 1)

with the voltage set to zero yields charge as a function of the deflection:

$$Q = \frac{3d_{31}Ewh\delta}{4L}. \quad (3)$$

The comparison of this expression with the COMSOL results is given in Table 2. There appears to be a factor of 2 difference in the results. This difference is an area for future investigation, and is suspected to be an error in Reference 1. The value of displacement used was equal to the displacement resulting from the application of 2 kV with zero applied force.

**Table 2. Comparison of numerical and analytical results for displacement**

Inputs	Outputs	
Displacement (mm)	Numerical Charge (nC)	Analytical Charge (nC)
32.812	50.2	25.0

Given the generally good agreement between the bimorph analytical expressions and the numerical model, we compared the results for an analytical expression of displacement resulting from an applied voltage to the corresponding numerical results. To our knowledge, this is the first derivation of this relationship. Modeling the piezoelectric constant as  $d_{31} + zd_{31}$  in a single layer unimorph, we found

$$\delta = \frac{d_{31}'L^2}{2h} V. \quad (4)$$

Several variations of voltage and film thickness were tested, and all results agreed to at least five significant figures. As an example, using a 70  $\mu\text{m}$  thick film with  $d_{31} = 5 \times 10^{-7} \text{ C/J}$  (a value typical of what we expect based on  $d_{31} = 28 \times 10^{-12} \text{ C/N}$ ) yielded a deformation of 54.7 mm at the end of an 87.5 mm film. However, this simplified model does not account for the internal field that results from the strain caused by the bending of the film. When the numerical model includes this effect, the deformation is reduced by approximately 14%. This effect clearly warrants further investigation and we will attempt to include it in the analytical model.

The multiphysics design tool is nearing completion. Previously, several models of one dimensional film with varying electrode spacing were simulated. By examining the curvature, the 2<sup>nd</sup> derivative of the deformation, along the surface of the electrode, the optimal spacing between electrodes can be determined. The result was that the electrodes need to be spaced 1mm or less to maintain a continuous curvature without any drastic deviations. For the 2-D model, the electrodes will be in a pattern consisting of rings and arms to set the desired curvature. The optimization of the electrodes requires an algorithm developed to determine the locations of the electrodes based on inputs such as the number of rings and arms, electrode spacing, and size of the outside. MATLAB was used to develop the algorithm since it is the central hub of the integrated software model. Figure 1 is the result from a single run of the algorithm.

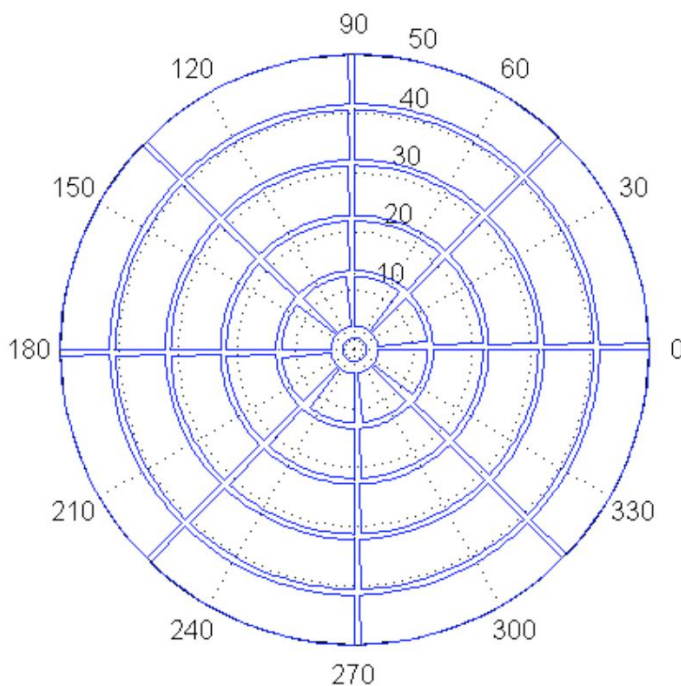


Figure 1. Example electrode pattern from script within the multiphysics tool

### ***Experimental Testing***

Testing has taken two separate directions. The first area is exploration of the deformation response of the film to an applied voltage, and the approach was described in the previous quarterly report. The films have been subjected to a broad series of tests described below. The second area is exploration of the charge generation response of the film to an applied load. Both

tensile and bending loads have been applied and response measured. However, the bending loads have not been as well controlled so the results are not as repeatable.

## Applied Voltage

During this period the experimental setup included a digital to analog convertor (DAC), which enabled computer control of the applied voltage as well as measurement of the deformation as previously described. One of the first tests was application of a 0 – 2 kV square wave, which is shown in Figure 2 (top). The pronounced ringing was due to the mechanical vibration of the excess portion of the film below the electrode. After trimming the film to remove the excess, the ringing was virtually eliminated Figure 2 (bottom).

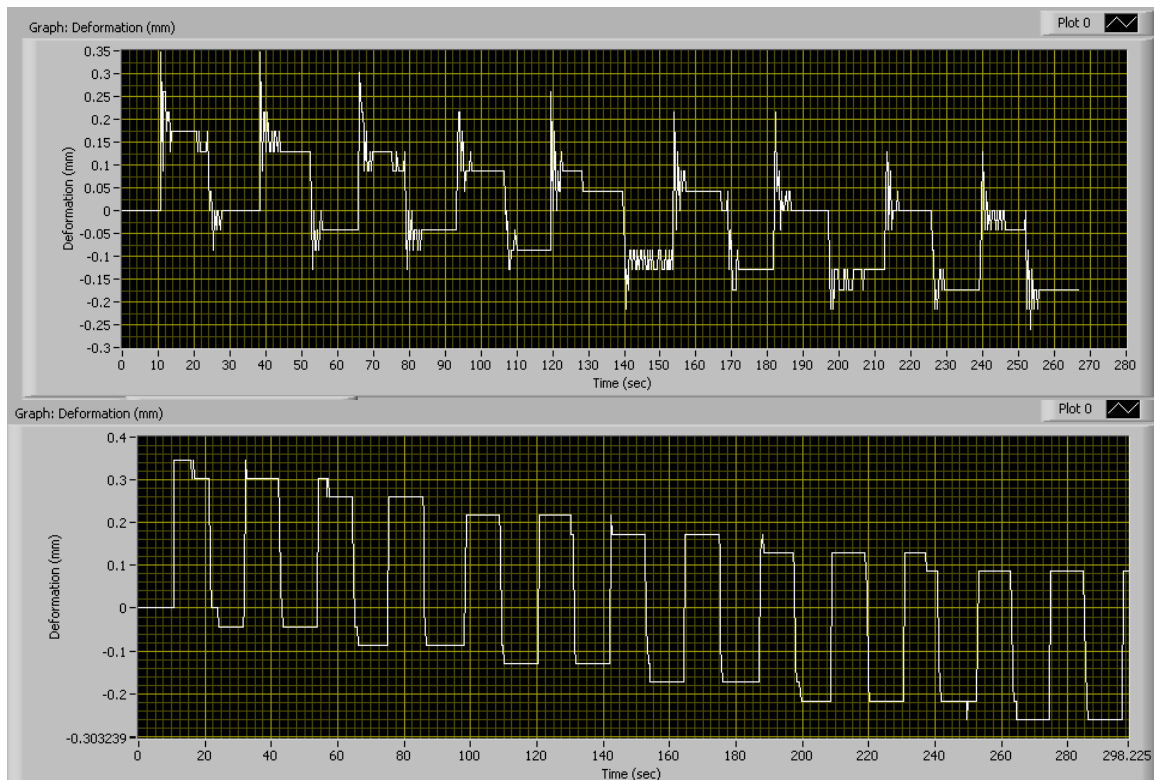


**Figure 2. Tip response to alternating 0 and 2kV voltage, 10.6 cm length (above) and 3.8 cm length (below)**

From this result, it can be seen that there is a significant amount of drift in the film. The remaining data taken during this test (which lasted almost 900 sec) show the drift continues until the deformation at 0 V is almost 0.5 mm. A similar pattern was observed when a constant 3 kV was applied to the film. Repeated tests have produced somewhat inconclusive and inconsistent results. These results include what appears to be a spontaneous reversal of the poling direction of the film, significant change in deformation in the absence of applied voltage, and changes in the responsivity of the film to applied voltage. We have engaged in a systematic study to understand the cause of these results and correlate the response with the experimental conditions. Initial indications include temperature of the film may be a factor. Measured temperatures reached 46 °C. However, published results indicate thermal effects on the piezoelectric coefficients are fairly minor until temperatures of 80-140 °C (depending on the polymer) are reached.<sup>2</sup> Testing using LED illumination rather than incandescent illumination is being

performed, but thermal effects will need to be revisited. It also appears that polymer creep may play a role in the behavior.

## Applied Load

The applied load testing has used an ORTEC 439 Digital Current Integrator to measure the charge generated by applying various loads to the films. Two configurations have been used in which the applied loads have been in the plane of the film (tensile test) and perpendicular to the surface of the film (bending test). The tensile testing has been performed using the NeXolve Instron tensile tester. An example is shown in Figure 3. As the jaws holding the ends of the film separate vertically, charge is generated on the two electrodes by the piezoelectric response of the film. The charge is collected by the ORTEC 439, which outputs a digital pulse for each 100 pC of charge. These pulses are counted and recorded as a function of time. Simultaneously, the Instron is recording the applied load and extension of the film as a function of time. By synchronizing the times (the end of the test was the sharpest event), the charge vs. load curve was determined.

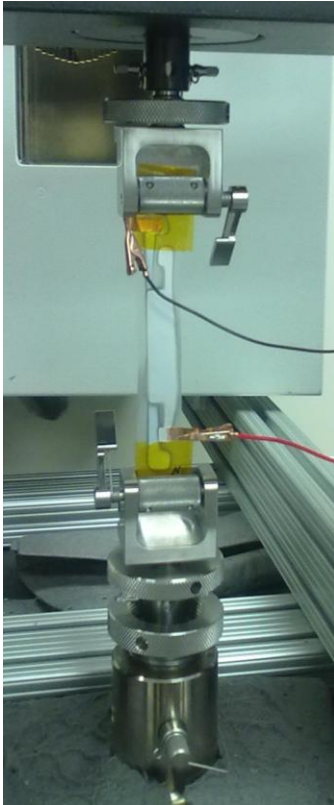


**Figure 3. Film loaded in Instron tensile tester with connections to the current integrator**

Following the constituent equations given in Smits,

$$\begin{aligned} S_1 &= s_{11}^E T_1 + d_{31} E_3 \\ D_3 &= d_{31} T_1 + \epsilon_{33}^T E_3 \end{aligned} \quad (5)$$

$E_3$  and  $D_3$  are the electric and displacement fields, respectively, in the  $z$ -direction (thickness of the film), and  $s_{11}^E$  is the compliance in the  $x$ -direction (long direction, which is the direction of the load). Stress ( $T$ ) and strain ( $S$ ) are given by

$$S_1 = \frac{\Delta x}{L_f} \quad T_1 = \frac{F}{hw_f}, \quad (6)$$

with symbols  $L_f$ , length of film;  $w_f$ , width of film;  $h$  thickness of film;  $L_e$ , length of electrode;  $w_e$ , width of electrode;  $F$ , applied load; and  $\Delta x$ , extension of film under load.

With the current integrator connected, the electrodes are effectively connected due its very small input impedance, so  $E_3 = 0$ , and

$$\Delta x = \frac{L_f s_{11}^E}{hw_f} F \quad \text{or} \quad s_{11}^E = \frac{hw_f}{L_f} m_{x-F}, \quad (7)$$

where  $m_{x-F}$  is the slope of the extension-load curve. The compliance is equal to the reciprocal of Young's modulus ( $E$ ), which is often referenced. An example set of data is shown in Figure 4. As expected, the result is very linear. The elastic modulus determined from this graph is 1.52 GPa, which is reasonably consistent with average literature values of PVDF of 1.65 GPa.<sup>3</sup>

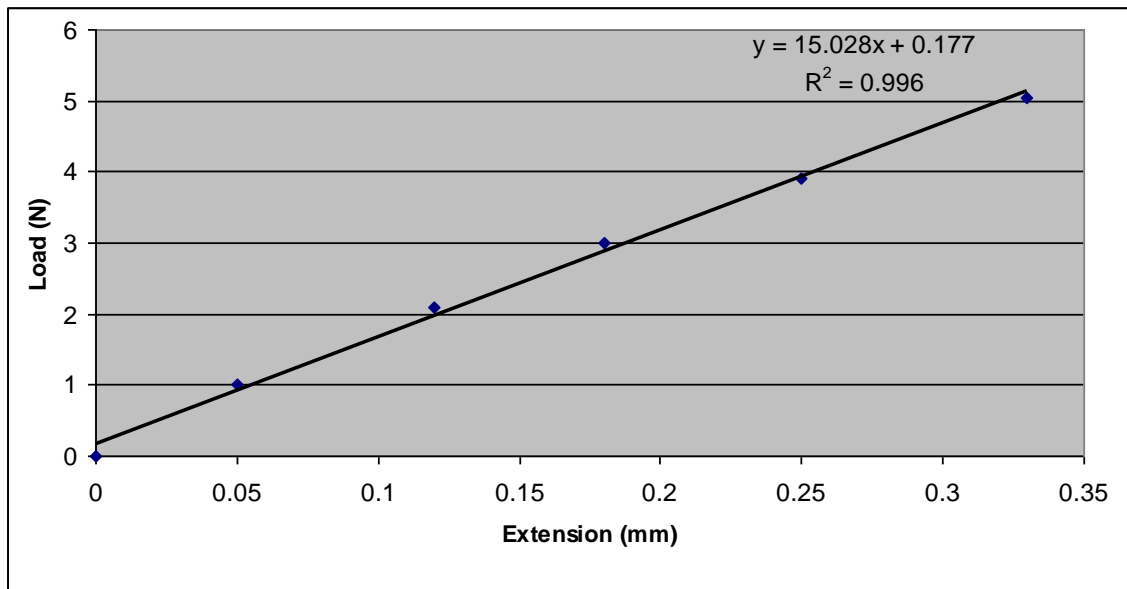


Figure 4. Load - extension graph for 69 um film loaded at 0.05 mm/s

The bound surface charge density developed as a result of the strain is  $\sigma_b = P$ , where  $P$  is the polarization.<sup>4</sup> By definition,  $D = P + \epsilon_0 E$ , so  $\sigma_b = d_{31} T_1 = Q/A_e = Q/L_e w_e$ . Here  $Q = kC$ , where  $k$  is the current integrator setting (100 pC/count) and  $C$  is the number of counts. Thus,

$$Q = d_{31} T_1 A_e = d_{31} (L_e w_e) / (L_f w_f) \quad (8)$$

and

$$C = d_{31} \frac{L_e w_e}{k h w_f} F \quad \text{or} \quad d_{31} = \frac{h w_f}{k L_e w_e} m_{C-F}, \quad (9)$$

where  $m_{C-F}$  is the slope of the counts vs. load curve. The pulse count vs. load graph is also very linear, as shown in Figure 4. The calculated value of  $d_{31}$  is 12.5 pC/N (or pm/V). This is somewhat lower than the values seen in the literature of 15-28 pC/N, but very reasonable.

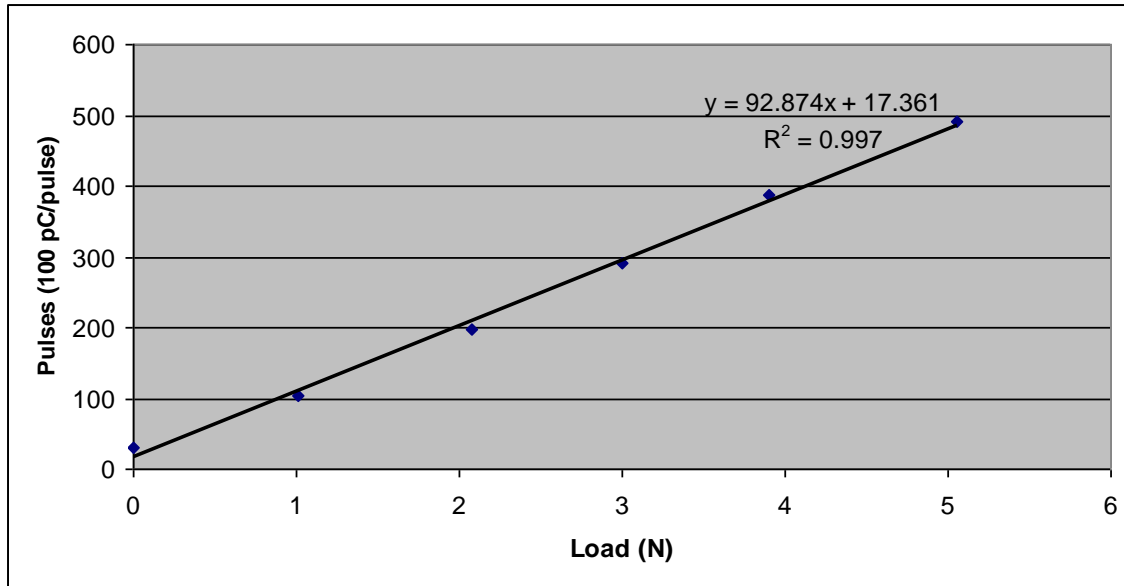


**Figure 5. Current integrator counts vs. applied tensile load for the same test as Figure 4**

The first round of testing was primarily to explore the test procedure. Based on this exploratory testing, we have identified the appropriate test conditions, such as strain rate. This testing occurred near the end of the quarter, and additional tests are scheduled for the first week of next quarter.

The second set of tests with applied loads involved applying a lateral load, which resulted in the film bending. This was preliminary testing to explore test procedures and shown in Figure 7. As before, testing was started using the bimorph sample fabricated from two films bonded together with poling directions anti-parallel. From Eq. 1, a linear relationship is expected between the displacement and the charge generated. However, Figure 8 shows that there is a quadratic component to the charge production. This could be due to the presence of the gradient in the piezoelectric coefficient, since we have not yet developed an analytical model for the charge generation including the gradient, as well as other effects not accounted for. However, ignoring the quadratic component for present, a linear fit using the measured value of  $E = 1.6$  GPa yields a  $d_{31}$  value of 11 pm/V, which is in agreement with the value found from the tensile testing. Using the slopes from the upper half of the curve and the lower half curve,  $d_{31}$  values in the range 8 – 15 pm/V are obtained.

### Dielectric Constant

Although the dielectric constant is not used in the analysis of the experimental data, it is used in the COMSOL modeling. Therefore, a quick measurement of the dielectric constant was performed. A circuit was built as shown below. The AC voltage source was the NI 9264 analog output. The source was configured to output 0 - 10 V square waves. The voltage measurement was done using the Agilent oscilloscope. The resistor was the 49.9 kohm precision resistor. The capacitor was the 69  $\mu$ m film sample E.

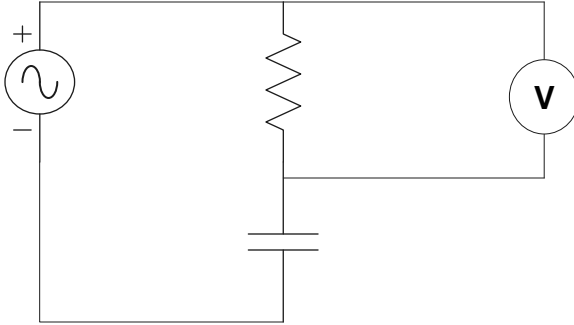
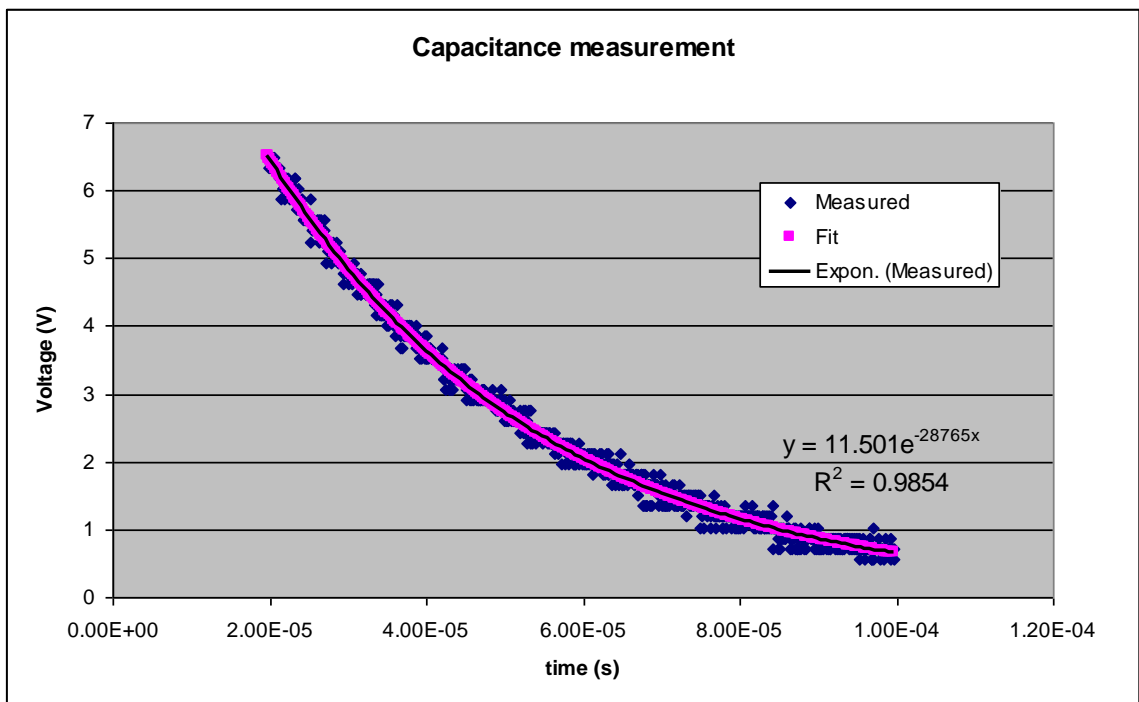


**Figure 6. Schematic diagram for capacitance measurement**

The oscilloscope recorded the decay of the voltage as the voltage source transitioned from 10 V to 0 V. After allowing transient from analog output to decay for 20  $\mu$ s, voltage vs time is shown in the figure below. The exponential decay provides excellent fit to the data.



From  $\tau = R/C$ , the capacitance can be determined to be 731 nF. Then using the capacitance of a parallel plate capacitor,

$$C = \epsilon_r \epsilon_0 \frac{A}{d}, \tag{10}$$

and the dimensions of the electrodes ( $L= 52$  mm,  $w= 11$  mm,  $d=69$   $\mu$ m), the dielectric constant  $\epsilon_r=10.0$ . This is in reasonable agreement with the value found in the literature.<sup>3</sup>

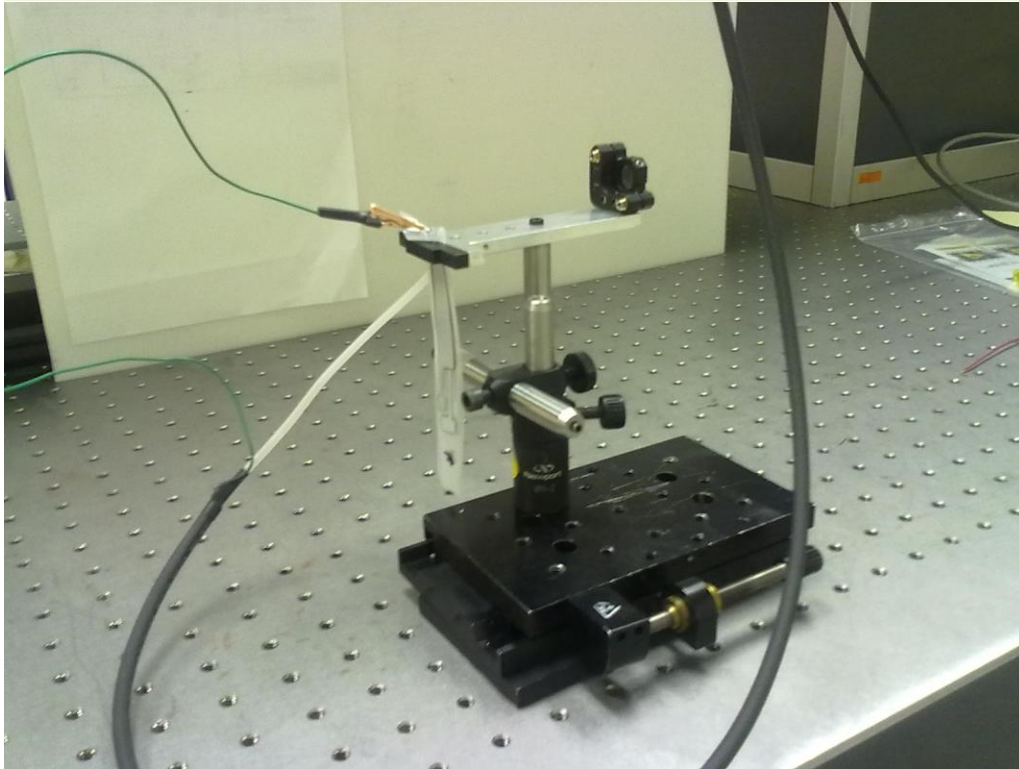


Figure 7. Test setup measuring response to lateral loads

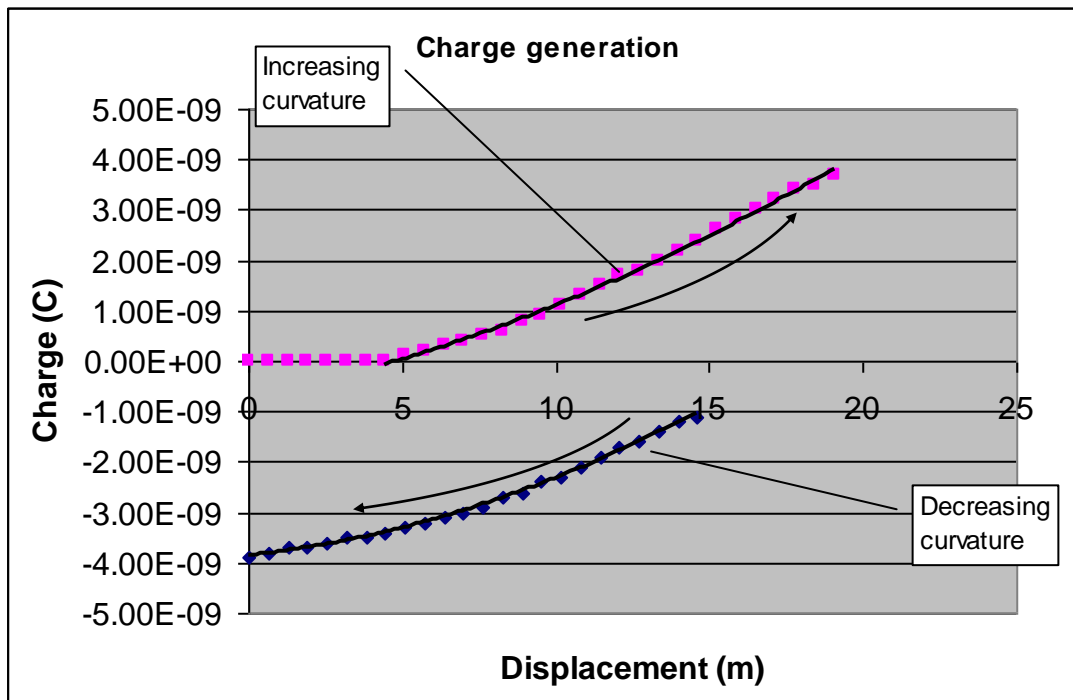


Figure 8. Charge generated by bending bimorph strip

## Material Crystallinity

Films manufactured during the previous two quarters were examined further by NeXolve

using differential scanning calorimetry (DSC) to quantify the relative amounts of beta and alpha crystal phases present in the film samples. The beta crystal phase is piezoelectrically active while the alpha phase is not. DSC can determine the relative amounts of each crystal phase, although NeXolve is not currently set up to determine the absolute material fraction of each phase. The proportions of each crystal phase were measured and can be seen in Table 3.

**Table 3: Relative amounts of Beta and Alpha Crystal phases in PVDF copolymer films.**

Sample	Film Thickness	Beta Crystal	Alpha Crystal	Total Crystallinity	Beta Crystal	Alpha Crystal
Identification	um	J/g	J/g	J/g	%	%
081810-1010	54	31.87	62.86	94.73	33.64%	66.36%
081810-1012	55	64.41	27.95	92.36	69.74%	30.26%
081810-1014	55	33.99	61.71	95.70	35.52%	64.48%
BF100908.004	41	49.34	6.295	55.63	88.69%	11.31%
BF100908.003	75	48.95	8.449	57.39	85.28%	14.72%
BF100908.005	69	49.05	6.425	55.47	88.42%	11.58%
aftertesting- BF100908.005-A	69	50.05	6.551	56.60	88.43%	11.57%
aftertesting- BF100908.005-E	69	50.12	7.212	57.33	87.42%	12.58%

The first three samples (green) are examples of films from other programs that have the incorrect amount of beta and alpha crystal phases needed to be piezoelectrically active, while the other samples are films produced for this program that exhibit the proper crystal phases. The samples in orange are from the same film. Sample BF100908.005 was tested before poling, and after poling and electrical/mechanical testing was performed. These films did not exhibit a significant change in crystallinity before poling and after testing.

## Results and Discussion

The multiphysics design tool is integrating well and will enable an empirical approach to understanding the behavior of the films. The next step in the tool development is determination of the parameters to extract from the optical analysis in order to compute the voltages needed to achieve the desired shape. This task will be closely tied with development of the diagnostic system optical design, which will begin early in the next quarter. The need for an analytical model for charge generated given an applied load or deformation is needed for understanding behavior of the film and under development.

On the experimental side, the biggest challenge is developing an understanding of the long term behavior of the films under applied voltages. In addition, the effect of relatively low heat levels is not consistent with our expectations based on results from the literature. We have begun a systematic study to determine the conditions and causes of the anomalous behavior. The results obtained by tensile testing have been consistent with values from the literature as well as values from other testing performed on this program. The next step will be assessing a variety of sample under better defined conditions. The bending tests will be performed using the unimorph films with a motorized translation stage to assess the impact of translation speed on the measurements and to improve repeatability.

## Conclusions

The multiphysics design tool is progressing according to plan. At the beginning of the quarter, the experimental work was behind schedule but is catching up. However, there have been unexpected challenges in understanding the properties of these materials. The focus for the next quarter will be on completing the material characterization and beginning the design of the diagnostic optical system.

---

<sup>1</sup> Jan G. Smits, Susan Il Dalke, and Thomas K. Cooney, “The constituent equations of piezoelectric bimorphs,” *Sensors and Actuators A*, **28**, pp. 41-61 (1991).

<sup>2</sup> Tim R. Dargaville, Mathias C. Celina, Julie M. Elliott, Pavel M. Chaplya, Gary D. Jones, Daniel M. Mowery, Roger A. Assink, Roger L. Clough, and Jeffrey W. Martin, “Characterization, Performance and Optimization of PVDF as a Piezoelectric Film for Advanced Space Mirror Concepts,” Sandia Report SAND2005-6846 (2005).

<sup>3</sup> MatWeb Material Property Data, Overview of materials for Polyvinylidene Fluoride (PVDF), Molded/Extruded, <http://www.matweb.com/search/DataSheet.aspx?MatGUID=a011f8ccf4b448a19246773a32085094&ckck=1>, Accessed 11 March 2011.

<sup>4</sup> Paul Lorrain and Dale R. Corson, *Electromagnetic Fields and Waves*, W.H. Freeman and Co., San Francisco, (1970).